Dear Reviewers:

We would like to sincerely thank you for your insightful and constructive comments, which have been very helpful to us in improving our manuscript. We carefully considered and fully addressed all comments. Below are the detailed point-by-point responses to the review comments. For clarity, the referees' comments are listed in black italics, and our responses and changes in the manuscript are shown in blue. We also mention where we made necessary changes in the revised manuscript by indicating page and line numbers in our responses. Please find below our point-by-point replies to your comments.

Response to Reviewer #2

A smart DSR retrieval scheme was developed and applied over the Tibetan Plateau. The effect of complex terrain in this region was investigated. The research looks interesting and the results look robust.

Author Response: Thank you very much for your positive comments. All comments were helpful for improving our manuscript. We carefully revised the manuscript and made the following point-by-point revisions according to your suggestions.

Major concerns:

1. *It is not clear how to derive water vapor content, whether it is derived from meteorological observations of temperature or relative humidity or directly from MODIS product.*

Author Response: Thank you for this comment. The water vapour content was derived based on air temperature and relative humidity, which are from the China Meteorological Forcing Dataset (CMFD). The precipitable water w (cm) is estimated from relative humidity RH (%) and air temperature T_{air} (K) by a semiempirical formula (Yang et al., 2006; Yang et al., 2010):

$$w = 0.00493RH{T_{air}}^{-1}\exp(26.23 - 5416{T_{air}}^{-1})$$

Relevant statements have been added in the revised manuscript. (P28, L618-L620).

'The precipitable water w (cm) is estimated from relative humidity RH (%) and air temperature T_{air} (K) by a semiempirical formula (Yang et al., 2006; Yang et al., 2010):

$$w = 0.00493RH{T_{air}}^{-1}\exp(26.23 - 5416{T_{air}}^{-1}), \quad \text{(A22)'}$$

The references are as follows:

Yang, K., Koike, T., and Ye, B.: Improving estimation of hourly, daily, and monthly solar radiation by importing global data sets, Agric. For. Meteorol, 137, 43-55, 10.1016/j.agrformet.2006.02.001, 2006a.

Yang, K., He, J., Tang, W., Qin, J., and Cheng, C. C. K.: On downward shortwave and longwave radiations over high altitude regions: Observation and modeling in the Tibetan Plateau, Agric. For. Meteorol, 150, 38-46, 10.1016/j.agrformet.2009.08.004, 2010a.

2. *It is not clear how to estimate turbidity from AOD at 550nm, my understanding is that Angstrom wavelength exponent over land is not good enough for the extrapolation.*

Author Response: Thank you for this comment. In this study, turbidity was estimated via AOD at 550 nm and the Angstrom wavelength exponent, with the Angstrom wavelength index assumed to be 1.3. The Angstrom wavelength exponent varies with aerosol type, aerosol size, and climate conditions. Therefore, the Angstrom wavelength exponent over land is not sufficient for extrapolation. Nevertheless, the method adopted in this study has been used by several studies (Kim, 2004; Yang et al., 2006; Huang et al., 2018), and the derived DSR has also been validated with high accuracy. This proves that the method is suitable for some study areas. Moreover, due to the high altitude of the TP, the air is clean, and the aerosol load is low (Xin et al., 2007; Xia et al., 2008). The uncertainty caused by the Angstrom wavelength exponent is relatively small compared to other regions (Chen et al., 2012; Roupioz et al., 2016). A reliable Angstrom wavelength exponent may further improve the accuracy of the estimated DSR. However, this is still a challenging task, and more detailed work needs to be carried out in the future.

The references are as follows:

Kim, D.-H.: Aerosol optical properties over east Asia determined from ground-based sky radiation measurements, Journal of Geophysical Research, 109, 10.1029/2003jd003387, 2004.

Yang, K., Koike, T., and Ye, B.: Improving estimation of hourly, daily, and monthly solar radiation by importing global data sets, Agric. For. Meteorol, 137, 43-55, 10.1016/j.agrformet.2006.02.001, 2006a.

Huang, G., Liang, S., Lu, N., Ma, M., and Wang, D.: Toward a broadband parameterization scheme for estimating surface solar irradiance: Development and preliminary results on MODIS products, Journal of Geophysical Research: Atmospheres, 123, 12,180-112,193, 10.1029/2018jd028905, 2018.

Xin, J., Wang, Y., Li, Z., Wang, P., Hao, W. M., Nordgren, B. L., Wang, S., Liu, G., Wang, L., Wen, T., Sun, Y., and Hu, B.: Aerosol optical depth (AOD) and Ångström exponent of aerosols observed by the Chinese Sun Hazemeter Network from August 2004 to September 2005, Journal of Geophysical Research, 112, 10.1029/2006jd007075, 2007.

Xia, X., Wang, P., Wang, Y., Li, Z., Xin, J., Liu, J., and Chen, H.: Aerosol optical depth over the Tibetan Plateau and its relation to aerosols over the Taklimakan Desert, Geophysical Research Letters, 35, 10.1029/2008gl034981, 2008.

Chen, Z., Shao, Q., Liu, J., and Wang, J.: Estimating photosynthetic active radiation using MODIS, Journal of Remote Sensing, 16(1), 25-37, 2012.

Roupioz, L., Jia, L., Nerry, F., and Menenti, M.: Estimation of daily solar radiation budget at kilometer resolution over the Tibetan Plateau by integrating MODIS data products and a DEM, Remote Sensing, 8, 10.3390/rs8060504, 2016.

The following reference was added to the revised manuscript:

Kim, D.-H. : Aerosol optical properties over east Asia determined from ground-based sky radiation measurements, Journal of Geophysical Research, 109, 10.1029/2003jd003387, 2004.

3. *It was stated by the authors the accuracy of the retrieval algorithm is highly dependent on the quality of input data, so it seems very necessary to do some sensitivity analysis on the uncertainty produced by potential errors of input products.*

Author Response: Thank you for this comment. The accuracy of the parameterization scheme depends on the quality of the input data to some extent. To further understand the effect of uncertainties in input variables on the accuracy of the DSR retrieval scheme, sensitivity analysis of the DSR to input variables is conducted (Fig. 9 and Fig. 10). As shown in Fig. 8, three points located in the west, north central, and southeast of the TP are randomly selected for sensitivity tests. The average of each input variable (including air temperature Tair, air pressure Pair, specific humidity SH, ozone layer thickness, aerosol optical depth AOD, surface albedo, cloud effective

radius CER and cloud water path CWP) for three randomly selected points is selected as the default value.

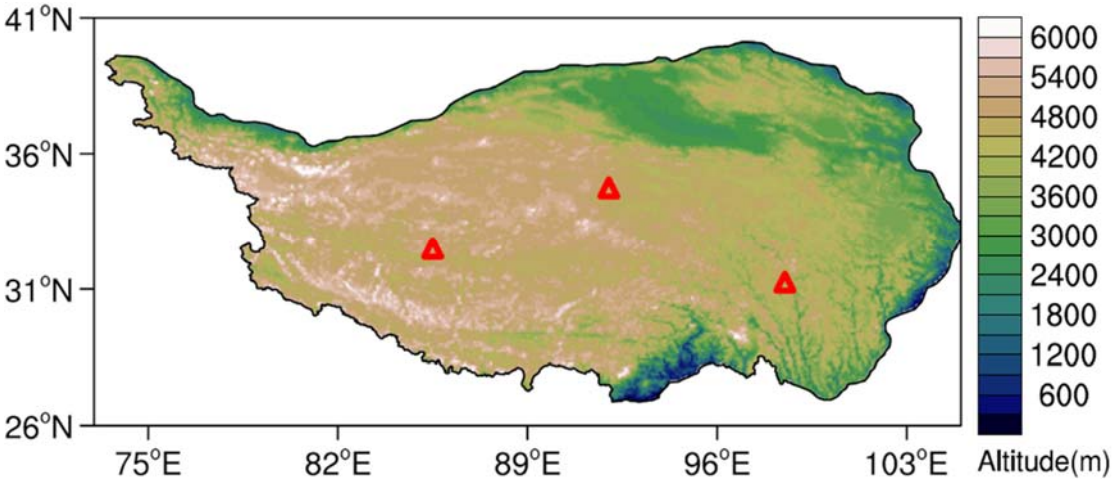

Figure 8. Locations of the three points (marked by red triangles) used to carry out sensitivity tests of the input data. The legend of the color map indicates the elevation above mean sea level in meters.

As shown in Fig. 9 and Fig. 10, in terms of changing trend and range, DSR has different responses to fluctuations of each input variable under different sky conditions. The sensitivity test results show that the DSR exhibits a positive correlation with Pair and ozone layer thickness and a negative correlation with Tair under both clear and cloudy conditions, with a nearly linear relationship (Fig. 9a, b, d and Fig. 10a, b, d). The DSR exhibits a negative correlation with SH and AOD with a nonlinear relationship under both clear and cloudy conditions (Fig. 9c,e and Fig. 10c,e). In addition, the DSR exhibits a positive correlation with CER and a nonlinear negative correlation with CWP under cloudy sky conditions (Fig. 10g and h). However, the DSR exhibits a linear positive correlation with surface albedo under clear sky conditions, while it displays a nonlinear positive correlation under cloudy sky conditions (Fig. 9f and Fig. 10f). This phenomenon indicates that multiple scattering effects occur between the atmospheric medium (aerosols and clouds) and the land surface (Ma et al., 2020).

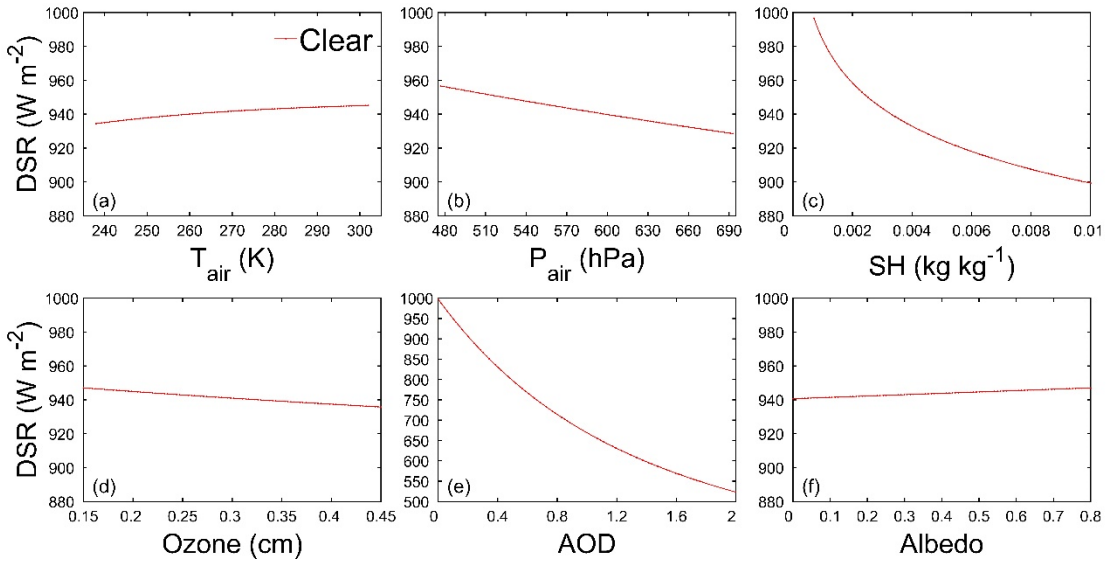

Figure 9. Sensitivity of DSR to (a) air temperature T_{air}, (b) air pressure P_{air}, (c) specific humidity SH, (d) ozone layer thickness, (e) aerosol optical depth AOD and (f) surface albedo under clear sky conditions.

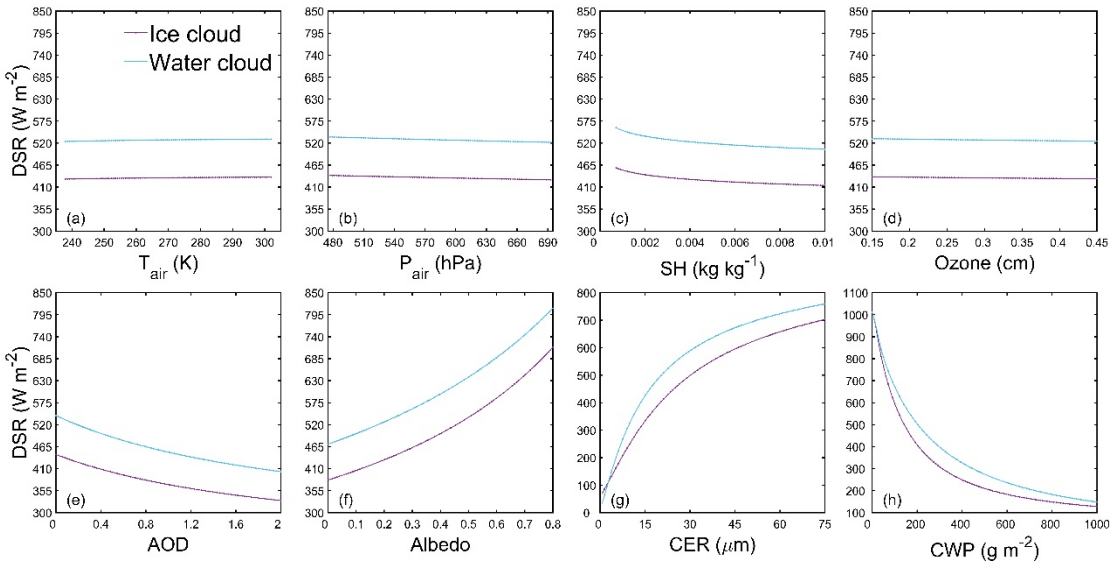

Figure 10. Sensitivity of DSR to (a) air temperature T_{air}, (b) air pressure P_{air}, (c) specific humidity SH, (d) ozone layer thickness, (e) aerosol optical depth AOD, (f) surface albedo, (g) cloud effective radius CER and (h) cloud water path CWP under cloudy sky conditions for ice clouds (purple line) and water clouds (blue line).

Moreover, the fluctuating range of input variables within one standard deviation (1σ) and the induced DSR fluctuation under different sky conditions are summarized in Table 6. Under clear sky conditions, the DSR is highly sensitive to AOD and SH and only slightly sensitive to other input variables. The AOD and SH within 1σ correspond to ranges of approximately 0-0.23 and 0.0004-0.0047 kg kg^{-1}, respectively, which would lead to DSR fluctuating by approximately 100.6 W m^{-2} and 87.4 W m^{-2}, respectively. Other input variables only induce fluctuations in DSR smaller than 15 W

m^{-2}. Under cloudy sky conditions, the DSR shows significant sensitivity to CWP and CER, moderate sensitivity to albedo, SH and AOD, and slight sensitivity to other input variables. The CWP within the 1σ range would lead to DSR fluctuating by approximately 768.1 W m^{-2} and 526.7 W m^{-2} for ice clouds and water clouds, respectively. The CER within the 1σ range would lead to DSR fluctuating by approximately 212.2 W m^{-2} and 202.3 W m^{-2} for ice clouds and water clouds, respectively. The magnitude of DSR fluctuations induced by the remaining input variables is much smaller than that caused by CWP and CER. In addition, the sensitivity of DSR to albedo is higher under cloudy sky conditions than under clear sky conditions, while the sensitivity of DSR to AOD and SH is lower under cloudy sky conditions than under clear sky conditions.

Table 6. Fluctuating range of input variables within one standard deviation (1σ) and the induced DSR fluctuation under clear sky and cloudy sky conditions.

	Clear		Ice cloud		Water cloud	
Variables	Ranges of variables within 1σ	DSR fluctuation range (W m^{-2})	Ranges of variables within 1σ	DSR fluctuation range (W m^{-2})	Ranges of variables within 1σ	DSR fluctuation range (W m^{-2})
T_{air} (K)	264-282	2.6	263-282	1.3	271-288	1.1
P_{air} (hPa)	530-622	-12.0	537-633	-4.9	550-646	-5.7
SH (kg kg^{-1})	0.0004-0.0047	-87.4	0.0006-0.0059	-38.0	0.0035-0.0083	-17.34
Ozone (cm)	0.25-0.28	-1.3	0.25-0.30	-0.7	0.25-0.28	-0.6
AOD	0-0.23	-100.6	0.03-0.21	-19.7	0.06-0.23	-21.1
Albedo	0.09-0.32	1.8	0.08-0.35	82.9	0.06-0.29	65.7
CER (μm)	-	-	16.7-39.8	212.2	9.3-21.4	202.3
CWP (g m^{-2})	-	-	0-409.6	-768.1	29.8-351.1	-526.7

In general, the inputs of cloud parameters CWP and CER are crucial variables, and their sensitivities are consistently high. AOD, surface albedo and SH are of secondary importance, with moderate sensitivity. AOD and surface albedo are more sensitive to DSR estimation than SH. Tair, Pair and ozone layer thickness only have a slight sensitivity to DSR estimation, in which ozone layer thickness is the least sensitive. The sensitivity test results indicate that the uncertainties in the input data of cloud parameters, aerosol parameters, surface albedo, and water vapour content are important error sources in the estimation of DSR (Huang et al., 2020; Letu et al., 2020).

The above information has been added to the revised manuscript. (P22, L459-P24,

L513)

4. *It is necessary to validate retrievals under clear and cloudy conditions, which is helpful for understanding of the uncertainty sources.*

Author Response: Thank you for this comment. The validation results under clear sky and all-sky conditions have been added to the revised manuscript. In addition, the DSR estimation results under all-sky conditions were also validated at ten-day and monthly timescales. Relevant statements have been updated in the revised manuscript. (P11, L249-L253).

'As shown in Fig. 3a and 3b, at the instantaneous scale, the RMSE and R of the 1 km DSR under clear sky are 105.34 W m^{-2} and 0.76, respectively, while those of the 1 km all-sky DSR are 158.19 W m^{-2} and 0.70, respectively. The validation results of this study are not as good as those in other plain areas, where RMSE and R are usually approximately 60 W m^{-2} and 0.9 under clear skies, while those of all-sky conditions are approximately 100 W m^{-2} and 0.9, respectively.' (P11, L249-L253)

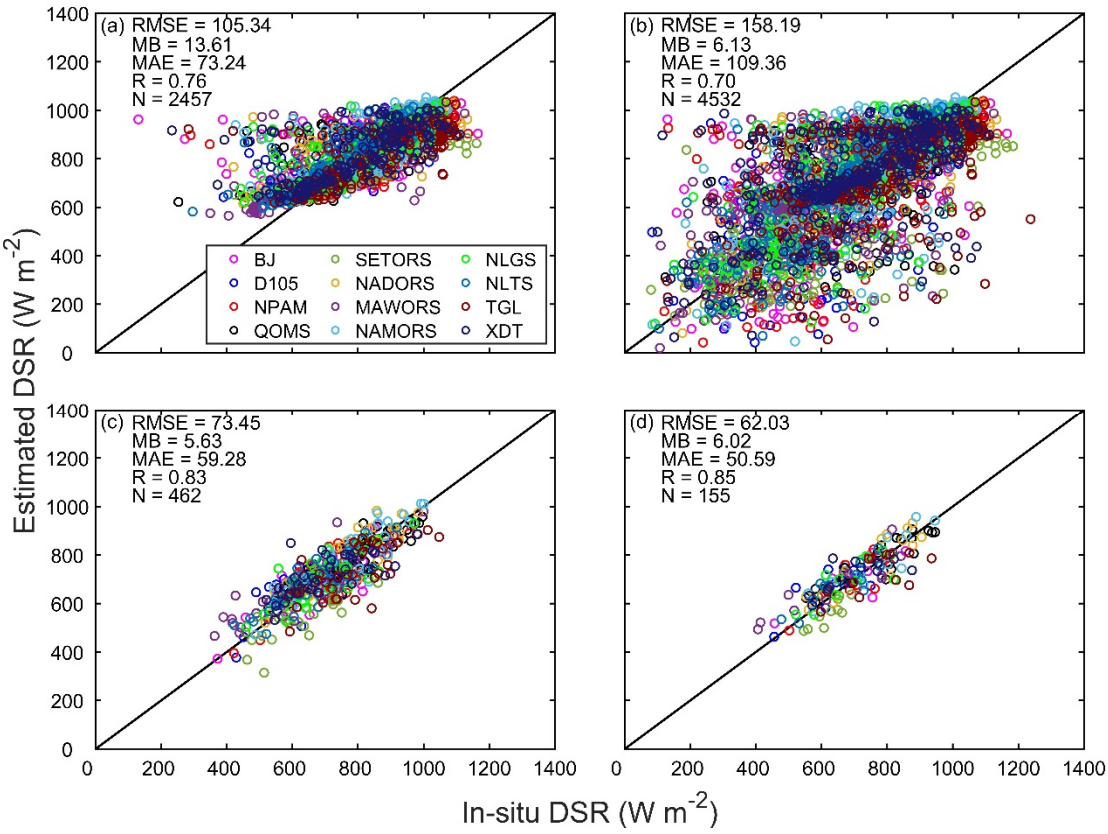

Figure 3. Validation results for the estimated DSR at (a and b) instantaneous scale, (c) ten-day scale and (d) monthly scale. Scatter plots (a) and (b) show the validation results of instantaneous DSR under clear sky and all-sky conditions, respectively. N indicates the number of points. The legend with different colors denotes twelve stations involved in the validation. The units of RMSE, MB and MAE are W m^{-2}.

5. *Measurements of DSR, especially the maintenance, data quality control, etc, should be introduced.*

Author Response: Thank you for this comment. Relevant statements have been added in the revised manuscript. (P8, L197-L203).

'Plausible value checks, time consistency checks and internal consistency checks were applied to ensure the accuracy and reliability of the observations. The original sampling data with high frequency were uniformly processed into 30 min and hourly average data by data loggers (e.g., CR3000, CR1000) (Campbell Sci., USA). To retain the observations in their original form as much as possible, no further postprocessing processes are taken, except for replacing outliers with missing values (NaN). Meanwhile, periodic inspection, maintenance and calibration are carried out by professional engineers at all stations.' (P8, L197-L203)